



ATMOSPHERIC PLASMA SPRAY COATING OF Ni-AL AND Al-Si ON AUSTENITIC STAINLESS-STEEL CASING WITH LIMITED SHORT SPRAY DISTANCE

Ahmad Sahid^{a,*}, Ekaviany Prajateljia^a, Ahmad Afandi^b

^aMaterial Science and Engineering Research Group
Faculty of Mechanical and Aerospace Engineering, Institut Teknologi Bandung
Jl. Ganesha 10 Bandung, Indonesia 40132

^bResearch Center for Physics, Indonesian Institute of Sciences
Gedung 440, Kawasan PUSPIPTEK Serpong, Banten, Indonesia 15314

*E-mail: ahmad.sahid.gerpasang@gmail.com

Masuk tanggal : 16-03-2021, revisi tanggal : 16-08-2021, diterima untuk diterbitkan tanggal 09-09-2021

Abstrak

Proses plasma spray atmosferik merupakan proses pelapisan yang banyak digunakan dalam aplikasi industri. Densitas dan kekuatan ikatan yang tinggi merupakan ciri utama dari proses ini dan diperlukan dalam hampir semua sifat lapisan untuk aplikasi-aplikasi khusus. Keterbatasan jarak semprot antara pistol nozel dan permukaan benda kerja pada saat proses plasma spray memerlukan modifikasi parameter proses standar. Pada penelitian ini, modifikasi parameter proses plasma spray lapisan Ni-Al dan Al-Si pada permukaan selubung baja tahan karat austenitik untuk mendapatkan hasil lapisan yang optimum. Lapisan diverifikasi dengan uji kekuatan ikatan tarik, uji keras, dan analisis struktur mikro. Dari modifikasi parameter yang dilakukan, penurunan kecepatan gerak pistol menunjukkan hasil yang paling optimum. Kekuatan ikatan tarik rata-rata yang diperoleh untuk lapisan Ni-Al dan Al-Si berturut-turut sebesar 9110 Psi dan 7283 Psi. Nilai kekerasan rata-rata yang diperoleh untuk lapisan Ni-Al dan Al-Si berturut-turut sebesar 77 HR_B dan 106 HR_H. Pengamatan struktur mikro lapisan Ni-Al menunjukkan struktur mikro yang lebih padat dibandingkan dengan struktur mikro lapisan dengan parameter standar. Untuk lapisan Al-Si, selain struktur mikro yang lebih padat, juga diperoleh fasa eutektik yang lebih proporsional dibandingkan dengan struktur mikro lapisan dengan parameter standar.

Kata Kunci: Plasma spray atmosferik, lapisan, Ni-Al, Al-Si, kecepatan lintas, kekuatan ikatan tarik, kekerasan

Abstract

The atmospheric plasma spray coating is a coating process that many used in industrial applications. High density and bond strength are the main features of this process. The limited spray distance between nozzle gun and workpiece surface during the plasma spray process requires standard process parameters modification. In the present study, an effort carried out a change of plasma spray process parameters of the Ni-Al and Al-Si coating on austenitic stainless steel casing for optimum results. Tensile bond strength, hardness, and microstructure tests were used to validate the coating. The Ni-Al and Al-Si layers had average tensile strengths of 9110 and 7283 Psi, respectively. The Ni-Al and Al-Si layers had average hardness values of 77 HR_B and 106 HR_H, respectively. When compared to the microstructure with standard parameters, the microstructure of the Ni-Al layer showed a denser microstructure. In addition to the denser microstructure of the Al-Si layer, a more proportional eutectic phase was obtained when compared to the microstructure of the layer with standard parameters.

Keywords: Atmospheric plasma spray, coating, Ni-Al, Al-Si, traverse speed, tensile bond strength, hardness

1. INTRODUCTION

The APS (atmospheric plasma spray) coating is a thermal spray coating method that is widely used for a variety of protective coatings, including thermal barrier, corrosion-resistant, and wear-resistant surfaces [1]. The plasma arc used as an energy source can generate a very high temperature from the inert gas plasma jet [2]. This capability allows all types of feedstock materials to be melted during the coating process. This extremely high temperature will be decreased by increasing distance from the arc, thus keeping substrate material remains cool and have little or no changes in its microstructure [3]. The heated feedstock materials will form a molten or semi-molten state before being accelerated and propelled toward the cleaned and blasted surface [2]. Upon impact to the surface, a mechanical bond is created, resulting in splats and build-up layers with lamellar structure. The layers will then be cooled down and solidified [2]. Compare to another spray method, this atmospheric plasma spray offers a higher temperature, produces high density and tensile bond strength, and has uniform integrity. These properties will only be achieved by maintaining good substrate preparation, control environment, and process parameter. Process parameter standard in APS mostly was provided by the manufacturer as a complete package with its machine. However, it only works on a particular condition, such as the free distance between the spray gun and substrate. Changes in the shape, size, and geometrical workpiece lead to the change of the APS process parameter.

Two types of coating materials, nickel aluminum (Ni-Al) and aluminum-silicon (Al-Si), were selected. Ni-Al is the most widely used coating material for bond coat and has better suitability to apply in almost substrate [4]. It is used as a material for restoring worn components and as bond coats for specific and general industrial applications. Ni-Al coatings are self-bonding to steel substrates and have excellent oxidation resistance up to 800 °C (1470 °F). Mechanically clad aluminum and nickel composites provide this Ni-Al powder [5].

Another feedstock material, Al-Si, is mostly used as a structural material due to its better characteristics in wear resistance, lower thermal expansion coefficient, and high strength to wear ratio [6]-[10]. Al-Si is produced using gas atomized powders of aluminum alloyed with 12 wt.% silicon. These materials are excellent general-purpose materials for salvaging and rebuilding aluminum and magnesium alloy parts.

Plasma sprayed aluminum-silicon coatings are also used for the repair of worn jet engine components and the dimensional restoration of jet engine components that have been worn during manufacture. Aluminum with 12% silicon is a simple eutectic system with a low melting point. Silicon reduces the melting temperature to 577 °C (1071 °F) while increasing fluidity, specific gravity, and the coefficient of thermal expansion. It also decreases the contraction associated with solidification. The silicon present in the material is virtually pure, acting to increase the hardness of coatings produced from these materials and improving abrasion resistance. Aluminum silicon powders produce coatings that are harder and slightly denser than pure aluminum powder layers [11]. The purpose of choosing two coating materials was not to compare their mechanical properties or microscopic structure, but to learn about the trend that occurs when parameter changes are made to the metal powder group. In the present work, several parameters were investigated to find out the optimum result of coating on the substrate with limited geometry, followed by mechanical testing and microstructural examination.

2. MATERIALS AND METHODS

2.1 Material

As received substrate material of austenitic stainless steel 321 and two types of coating material Ni-Al and Al-Si with -90+45 µm particle size distribution was used in the present work. The substrate was prepared by solvent cleaning and grit blasting with aluminum oxide at 120 psi pressure.

The chemical compositions of each material are shown in Tables 1, 2, and 3, respectively.

Table 1. Chemical compositions of stainless steel substrate AISI 321 (in wt.%) [12]

Element	Composition (wt.%)
C	0.08
Mn	2.00
Si	1.00
Cr	18.00
Ni	11.00
P	0.05
S	0.03
Ti	0.40 (min)
Fe	Balance

2.2 APS Process Parameter

The atmospheric plasma spray coating process parameter was prepared based on the equipment guidance manufacturer and then modified to match the geometric condition. This geometric condition only allows a maximum spray distance of 2 inches, which differs from the standard parameter's amount of 9 inches. It will also increase the temperature of the base metal's surface and limit the amount of deposited dust that escapes from the spray area. The process parameter was limited to power as an output from ampere and voltage, speed of traverse gun and rotation of the workpiece, and feed rate of the powder. This study was prepared in accordance with the criteria listed in Table 4. The parameter is applied to the Al-Si and Ni-Al coating materials as a system on the AISI 321 stainless steel substrate.

Table 2. Chemical compositions of nickel aluminum (Ni-Al) coating material [5]

Element	Composition (wt%)
Ni	Balance
Al	4.5

Table 3. Chemical compositions of aluminum silicon (Al-Si) coating material [11]

Element	Composition (wt%)
Al	Balance
Si	12

2.3 Tensile Bond Strength Test

AISI 321 was prepared as a workpiece substrate for tensile bond strength testing in accordance with ASTM C-633, standard test method for adhesion or cohesion strength of thermal spray coatings, using a rod-type specimen with a diameter of 1 inch and a length of 2.5 inches [13]. A universal testing machine (Shimadzu) was then used to examine the sample. This testing method is used to determine the adhesive strength between the coating and the

substrate, as well as the cohesive force within the coating. It had one coated surface and one blasted surface that were both sticky when combined with the adhesive film. All specimens were assembled in a special fixture before being cured in the oven. Following curing, excessive adhesion film was removed from the adjacent surface with grit abrasive paper or cloth. At room temperature, the specimen was mounted to the tensile testing machine with a fixture to allow for handling during the process. Each sample was tested until rupture occurred at a constant stress rate and crosshead travel. Each specimen's rupture surface was examined to determine the type of failure of each coating. If the failure occurs between the coating and the substrate, the strength is referred to as adhesive strength. If it occurs within the coating, the strength is referred to as cohesive strength.

2.4 Hardness Test

The hardness specimen was created using the ASTM E18-20 standard test methods for Rockwell hardness of metallic materials [14]. The sample measured 3 inches in length, 1 inch in width, and 0.2 inch in thickness. The sample was then examined using a Rockwell hardness testing machine (Matsuzawa) and the Rockwell H (HR_H) and B values (HR_B). The goal of this test was to see how parameter changes affected the hardness of the coating.

2.5 Metallographic Test

Metallographic specimens were prepared in accordance with ASTM E1920, the standard guide for metallographic preparation of thermal sprayed, with specimens measuring 3 inches in length, 1 inch in width, and 0.2 inch in thickness [15]. The sample was then examined under a 100X magnification optical microscope (Nikon Microphot-FX). The goal of this microstructure evaluation is to determine the impact of parameter changes on the structure of Ni-Al and Al-Si coatings.

Table 4. Atmospheric plasma spray parameter modification for Ni-Al and Al-Si coating materials applied on AISI 321 stainless steel casing substrate

Parameter	Specimen A1 / B1 ^a	Specimen A2 / B2	Specimen A3 / B3	Specimen A4 / B4	Specimen A5 / B5
Power (kW)	35	30	35	35	35
Spray Distance (inches)	4	2	2	2	2
Powder Feed Rate (lb/hr)	10	10	5	10	10
A traverse speed of gun (mm/s)	10	10	10	7.5	10
A rotation speed of workpiece (RPM)	60	60	60	60	160

3. RESULTS AND DISCUSSIONS

3.1. Tensile Bond Strength Test

The failure feature of the tensile bond strength test specimen is shown in Figs. 1 and 2 for Ni-Al and Al-Si coating, respectively. There are two modes of failure resulted; the first one is an adhesive failure where the coating failed between coating and substrate. The second one is a cohesive failure where the failure occurred within the coating [13]. Adhesive failure may occur between substrate and bond coat which remain the grey colour of the substrate after failure. The adhesive failure occurred in three different parameters, which was selected based on the most failure occur in one set of specimens as shown in Figure 1. While in Fig. 2, adhesive failure occurs between the coating and adhesive film, which remain white colour after failure or between adhesive film and substrate, which remain the white colour of the adhesive film after failure. The first one was in the standard parameter, either A1 or B1. The Second one was obtained by reducing 50% of the powder feed rate from 10 lbs/hr to 5 lbs/hr with a spray distance of 2 inches for both A3 and B3. This was the maximum space that was available due to the limited geometry of the casing. The last was obtained by reducing the 25% traverse speed of the gun from 10 mm/s to 7.5 mm/s with the same spray distance for specimens A4 and B4. In the meantime, cohesive failure was obtained when the parameter of the process was reduced power to 30 kW from 35 kW and increased RPM of the workpiece to 160 RPM from 60 RPM standard parameter. From these results, reducing powder feed rate and traverse speed led to adhesive failure, while reducing power led to cohesive failure.

Tensile Test Bond Strength results of Ni-Al and Al-Si coating are shown in Figs. 3 and 4, respectively. Reducing traverse speed from 10 mm/s to 7.5 mm/s and spray distance from 4 inches to 2 inches in both A4 and B4 resulted in the highest tensile bond strength. The same result was found during the deposition process powder feed rate affect the mechanical properties [16]. There was an optimum powder feed rate in a certain value for a specific type of coating. This was found clearly in specimen A4, which had the highest tensile bond strength value. The lower spray rate tends to be more homogeneous particle heated and improve bonding. In the meantime, the deposition rate will be slower. While reducing power from 35 kW to 30 kW with the same spray distance, 2 inches, obtained the lower result. This was related to unmelted and partially

melted particles that were found in the coating that led to low tensile bond strength [17].

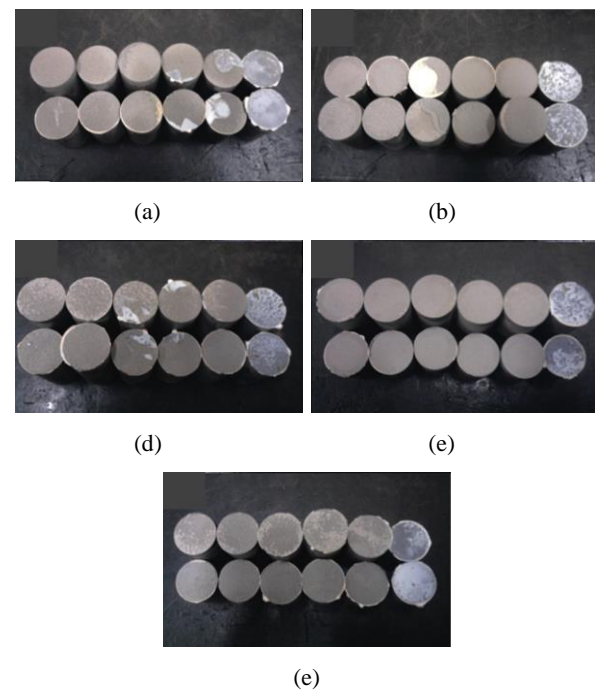


Figure 1. Failure feature of tensile bond strength Ni-Al coating specimen (a) A1, (b) A2, (c) A3, (d) A4, (e) A5

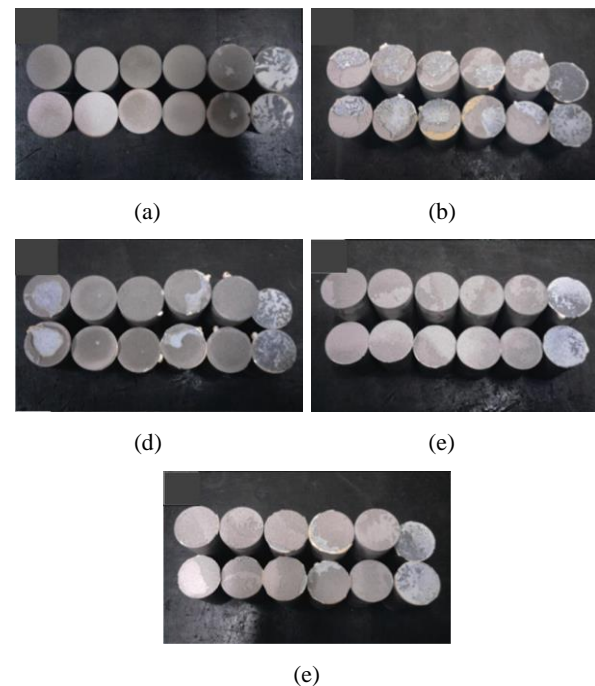


Figure 2. Failure feature of tensile bond strength Al-Si coating specimen (a) B1, (b) B2, (c) B3, (d) B4, (e) B5

Failure modes and tensile bond strength result indicated modification of spraying parameter affected to the result of coating properties. Reducing powder feed rate became a small amount of particle allowed heat absorbed almost of each particle and led to the optimum heating required by each particle.

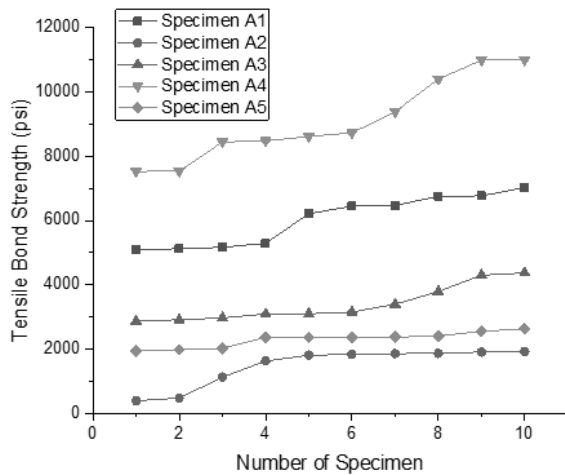


Figure 3. Tensile bond strength test result of Ni-Al coating

The other way was by making slower traverse speeds of the gun to maintain particle and workpiece heating at the same time. Having both in the same hot condition led particles and prepared substrate better mechanically bonded.

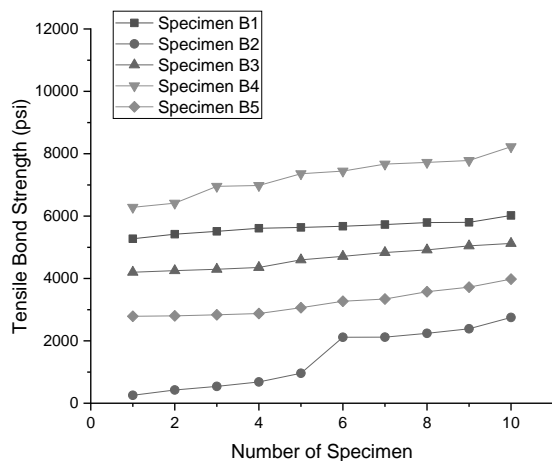


Figure 4. Tensile bond strength of Al-Si Coating

It was supported by the characteristic of Ni-Al particle that can create an exothermic reaction during processing, resulting in a quasi-metallurgical bond with stainless steel substrate. In Al-Si coating, higher bond strength was promoted by silicon element with 12% during the eutectic reaction.

3. 2. Hardness Test Result

Modification of parameter also affected the hardness properties of both coating, as shown in Fig. 5 and Fig. 6. In Ni-Al coating, the highest hardness value was obtained by reducing the traverse speed of gun from 10 mm/s to 7.5 mm/s (A4). However, reducing power and keeping the feed rate higher led to lower hardness results

(A2). The higher amount of heated particle with lower power led to partially melted particle that affect to the hardness value [18].

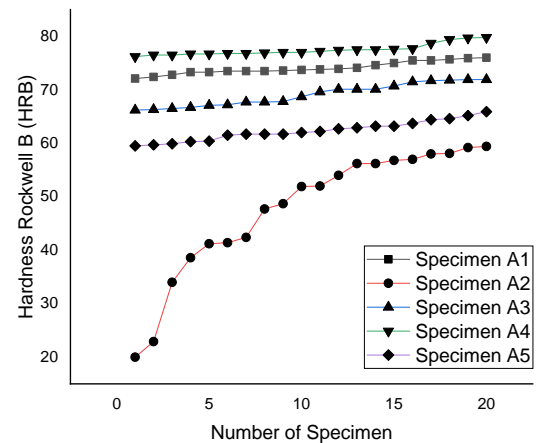


Figure 5. Hardness test result of Ni-Al coating

The exothermic reaction during spraying produced self-bonding of the dense and high structural integrity of Ni-Al coating [18]. Different from Ni-Al, in Al-Si, coating the amount of hardness is promoted by the number of eutectic phases that formed during spraying and high cooling rate [16]. Lesser spray distance, high heat input, and lower powder feed rate, a located particle of powder in the melting state that was suddenly cooled to ambient temperature, formed the more possibility to create the eutectic phase.

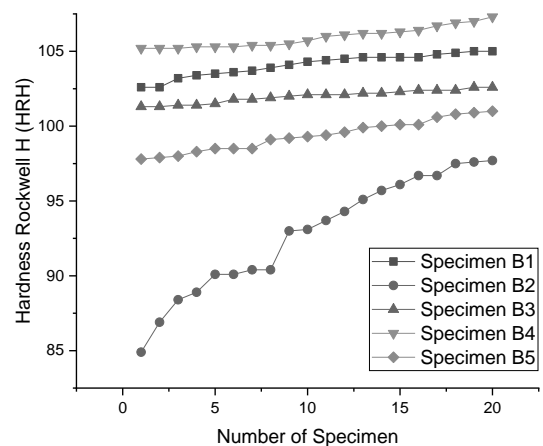


Figure 6. Hardness test result of Al-Si coating

3. 3. Microstructure

Microstructure examinations for Ni-Al and Al-Si coating were shown in Fig. 7 and Fig. 8, respectively. Starting from specimen A1 which followed the standard parameter, it has a moderate density of Ni-Al. A higher density of

Ni-Al was obtained for A4 from modification of spray distance and traverse speed of gun. However, lower density was also obtained for A2 from modification of power output. The degree of the high density of coating contributed to mechanical properties as confirmed in the above result of tensile bond strength and hardness, where dense coating resulted in high of mechanical properties [18].

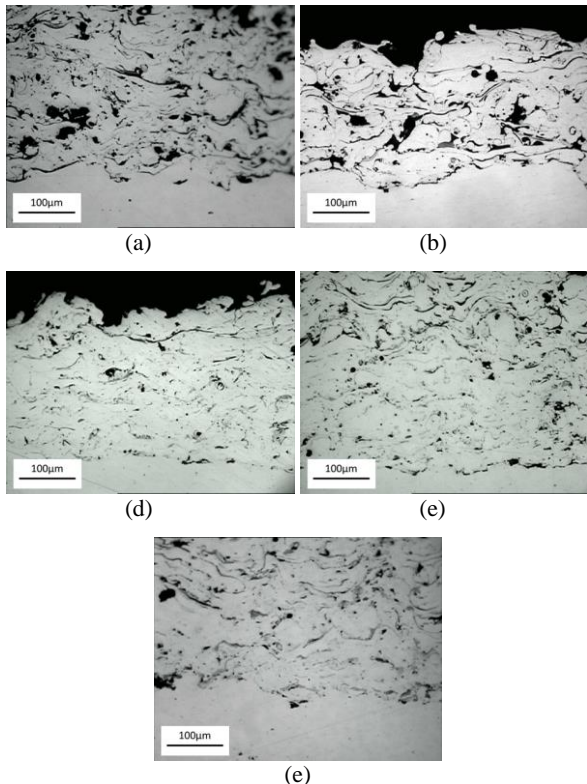


Figure 7. Microstructure of Ni-Al coating (a) A1, (b) A2, (c) A3, (d) A4, (e) A5

In another case, the initial Al-Si coating parameter B1 has a microstructure with the highest density and a small amount of eutectic phase. However, many pores were obtained for B2 with low power input. High density was mostly affected by heat input as a function of power. Besides the density, the eutectic phase was formed through a eutectic reaction during high solidification. It contributed to mechanical properties, mainly hardness and tensile bond strength, as discussed above [16]. It is confirmed by B4 that it has the highest mechanical properties.

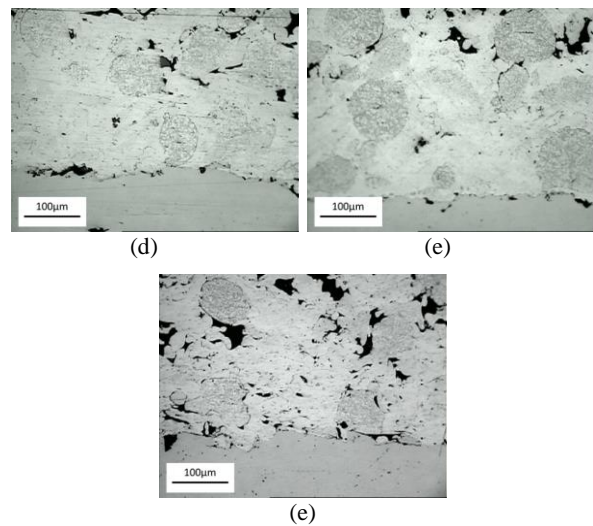
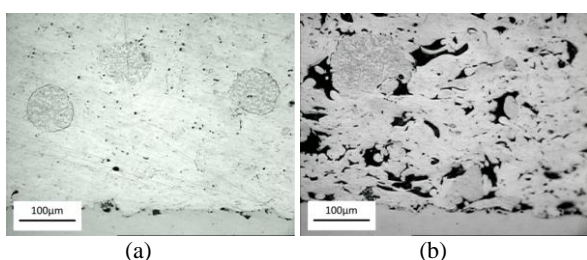


Figure 8. The microstructure of Al-Si coating (a) B1, (b) B2, (c) B3, (d) B4, (e) B5

4. CONCLUSIONS

To increase the mechanical properties and to improve the microstructure of the coating under a limited condition where the distance was less than guidance requirement, modification parameter by lowering traverse speed of gun could be considered to maintain the mechanical properties and improve the integrity of microstructure. Lowering traverse speed of gun showed better coating microstructure for both Ni-Al with less porosity and Al-Si with denser microstructure and moderate eutectic phase formation. This experimental research is useful for the industry that cannot invest in new equipment that was developed specifically for a limited purpose. This research was only focused on coating under the metal alloys group. Future work must identify the modification parameter to other groups, such as carbide, self-fluxing, abrasible, and ceramic coating.

ACKNOWLEDGEMENT

This research was supported by PT Nusantara Turbin dan Propulsi.

REFERENCES

- [1] A. Alian dan I. S. Jalham, "Abrasive wear resistance comparative study of plasma-sprayed steel by magnesium zirconate, aluminum-bronze, molybdenum, and mixtures of them as coating materials," *Arab. J. Sci. Eng. (Springer Sci. Bus. Media BV)*, vol. 31, pp. 27-34, 2006.
- [2] J. R. Davis dan D. & Associates, *Handbook of Thermal spray technology*, vol. 1, no. 6. ASM International, 2004.

- [3] G. Singh dan N. Bala, "Nanocomposites coatings by thermal spraying technique : A review," *Int. Conf. Adv. Futur. Trends Mech. Mater. Eng.*, pp. 643-648, 2012.
- [4] M. Zandrahimi, J. Vatandoost, dan H. Ebrahimifar, "Al, Si, and Al-Si coatings to improve the high-temperature oxidation resistance of AISI 304 stainless steel," *Oxid. Met.*, vol. 76, no. 3-4, pp. 347-358, 2011. Doi: 10.1007/s11085-011-9259-1
- [5] O. Metco, "Material product data sheet nickel-aluminum materials," 2020. <https://www.oerlikon.com> (accessed 16 Feb, 2021).
- [6] J. Clarke dan A. D. Sarkar, "Wear characteristics of as-cast binary aluminium-silicon alloys," *Wear*, vol. 54, no. 1, pp. 7-16, 1979. Doi: 10.1016/0043-1648(79)90044-9
- [7] Q. Xu, B. Gabbitas, dan S. Matthews, "Titanium compacts with controllable porosity by slip casting of binary powder mixtures," *Powder Technol.*, vol. 266, pp. 396-406, 2014. Doi: 10.1016/j.powtec.2014.06.042
- [8] M. Qian, D. Li, S. B. Liu, dan S. L. Gong, "Corrosion performance of laser-remelted Al-Si coating on magnesium alloy AZ91D," *Corros. Sci.*, vol. 52, no. 10, pp. 3554-3560, 2010. Doi: <https://doi.org/10.1016/j.corsci.2010.07.010>
- [9] M. Gurutze Pérez Artieda, A. Cortiella, N. R. Harlan, F. Zapirain, dan F. Zubiri, "Two step coating of a hypereutectic PM Al-Si alloy," *Mater. Lett.*, vol. 64, no. 13, pp. 1458-1461, 2010. Doi: 10.1016/j.matlet.2010.03.056
- [10] J. Wang, L. Kong, J. Wu, T. Li, dan T. Xiong, "Microstructure evolution and oxidation resistance of silicon-aluminizing coating on γ -TiAl alloy," *Appl. Surf. Sci.*, vol. 356, pp. 827-836, 2015. Doi: 10.1016/j.apsusc.2015.08.204
- [11] O. Metco, "Material product data sheet aluminum 12% silicon thermal spray powders," 2016. <https://www.oerlikon.com> (accessed 16 Feb, 2021).
- [12] J. R. Davis, *Metals Handbook Desk Edition*, Third. ASM International, 2001.
- [13] A. Standard, "ASTM C633-13: Standard Test Method for Adhesion or Cohesion Strength of Thermal Spray Coatings," *ASTM Int.*, pp. 4, 2008.
- [14] A. Standard, "ASTM E18-03: Standard test methods for rockwell hardness and rockwell superficial hardness of metallic materials," *Annu. B. ASTM Stand.*, no. 08b, pp. 1-37, 2003.
- [15] A. Standard, "ASTM E1920-03: guide for metallographic preparation of thermal sprayed coatings," no. 03, pp. 1-8, 2014.
- [16] M. Mrdak, B. Medjo, D. Veljić, M. Arsić, dan M. Rakin, "The influence of powder feed rate on mechanical properties of atmospheric plasma spray (APS) Al-12Si coating," *Rev. Adv. Mater. Sci.*, vol. 58, no. 1, pp. 75-81, 2019. Doi: 10.1515/rams-2019-0007
- [17] X. C. Zhang, B. S. Xu, S. T. Tu, F. Z. Xuan, H. D. Wang, dan Y. X. Wu, "Effect of spraying power on the microstructure and mechanical properties of supersonic plasma-sprayed Ni-based alloy coatings," *Appl. Surf. Sci.*, vol. 254, no. 20, pp. 6318-6326, 2008. Doi: 10.1016/j.apsusc.2008.03.148
- [18] L. Zhang, X. J. Liao, S. L. Zhang, X. T. Luo, dan C. J. Li, "Effect of powder particle size and spray parameters on the Ni/Al reaction during plasma spraying of Ni-Al composite powders," *J. Therm. Spray Technol.*, vol. 30, no. 1-2, pp. 181-195, 2021. Doi: 10.1007/s11666-020-01150-2

